Chapter D.5

Case Study 1: Integrated Analysis of a Humid Tropical Region – The Amazon Basin

Jeffrey E. Richey · Reynaldo Luiz Victoria · Emilio Mayorga · Luis Antonio Martinelli · Robert H. Meade

D.5.1 Towards an Integrated Analysis of the Amazon Basin

The Amazon makes for an excellent test case for developing a model of how hydrological and biogeochemical cycles function at the land surface on regional to continental scales. With an area of 6 Mkm^2 containing the largest stand of tropical rainforest in the world, it contributes 15% of the global freshwater discharged to the oceans, and condensational energy release from convective precipitation is of sufficient magnitude to influence global climatic patterns. Its major tributaries represent different climate, soil, and topographic regimes. It is large scale and represents a series of hydrological and chemical regimes that are not atypical of world rivers (Stallard and Edmond 1983). As much of the Amazon is mostly undisturbed by anthropogenic activity, it provides one of the few opportunities left to develop models of how basins function, against which future change can be assessed. It is also relatively well-characterised, even over large scales. Given the heterogeneous nature of precipitation and precipitation instrumentation, river discharge is perhaps the most robust integrator of the long-term hydrological properties of a drainage basin.

In this chapter we use a heuristic model construct to develop a synthesis of the coupling between the hydrological and biogeochemical cycles of the Amazon River system. Our emphasis is on the large-mesoscale to continental scale features of the river system, which would be compatible in scale with the land-atmosphere interfaces represented by general circulation models. This synthesis is based in large part on the work of the CAMREX (Carbon in the AMazon River EXperiment) project (Richey and Victoria 1996; McClain et al. 2001).

D.5.2 Coupling Hydrology, Organic Matter and Nutrient Dynamics in Large River Basins

The central premise of a large river basin model is that the constituents of river water provide a continuous, integrated record of upstream processes whose balances vary systematically depending upon changing interactions between flowing water and the landscape, and the interplay of biological and physical processes (Richey and Victoria 1996). That is, the chemical signatures of riverine materials can be used to identify different drainage basin source regions, reaches or stages, and can be tied to landscape-related processes such as chemical weathering and nutrient retention by local vegetation. The compositions of the particulate and dissolved materials carried by the mainstem result from initially similar rainwaters that have been uniquely imprinted by contact with almost every plant, animal and mineral in the basin.

A strategy for capturing these dynamics is to build multiple time- and space-scale integrated models of changes in the water flow and biogeochemistry of river basins as a function of changes in land use and land cover and regional climatology over the basin.

There are three components to this strategy. The first is to build a spatial model of the physiography of a region. The next step is to model the flow of water across the landscape and down river channels. A tributary basin analysis is predicated on determining the interannual patterns in precipitation and runoff; runoff pathways and soil residence time can lead to differences in how chemical species are mobilised and particulates eroded. The hydrology of a regional-scale river system can be modelled as a geospatially-explicit water mass balance within the basin contributing to stream flow and downstream routing. As such, a model can be divided into two major components. A "vertical" component, which calculates the water balance at each individual grid cell, and a "horizontal" component, which routes the runoff generated by each grid cell to the ocean. The separation into vertical and horizontal components also allows for an easy interface to treat non-point source and in-channel chemical processes separately.

The final step is to couple the spatial and hydrological models to models of the origin and transport of selected chemicals, or the biogeochemical models. Models developed for terrestrial systems typically pay little attention to exports to rivers, and the common paradigm used for soil organic matter compartments is based on turnover rates. Mayorga et al. (2000) proposed an integrated modelling framework aimed at quantitatively

describing the dynamics of organic matter cycling in mesoscale to large rivers by mechanistically tracking the evolution of organic matter from the land, through the river corridor, to the river (Fig. D.64). This model emphasizes the importance of physical and geochemical properties in controlling the preservation and fractionation of organic matter. The biogeochemical model is tightly coupled to spatially distributed models of water and sediment cycling and transport. The biological components of the border areas and the surface water act as filter systems to retain the organic carbon and nutrients for use in primary production and respiration. For instance, nitrogen leached as nitrate from terrestrial settings is often consumed in the process of denitrification when it enters the organic-carbon-rich environment of riparian zones. The organic matter from these producers is fuel for consumers in the water, sediments, and soil. This matter may be consumed near its place of production or transported downslope or downstream before being consumed. Because oxygen transport is reduced in water, oxygen availability can become limited in many areas in these settings, leading to the development of anaerobic conditions. Usually there are low concentrations of electron acceptors such as nitrate and sulfate, so fermentation and methanogenesis are the main anaerobic means of organic-matter degradation. The distribution of aerobic and anaerobic conditions in these areas determines the relative production of CO_2 and CH_4 (and CH_4 oxidation). These degradation reactions also involve the mineralisation of organic N, with the potential for production of N trace gases. Contrasts between non-flooding and flooding conditions can create conditions for the sequential mineralisation of organic N, aerobic nitrification, and anaerobic denitri-

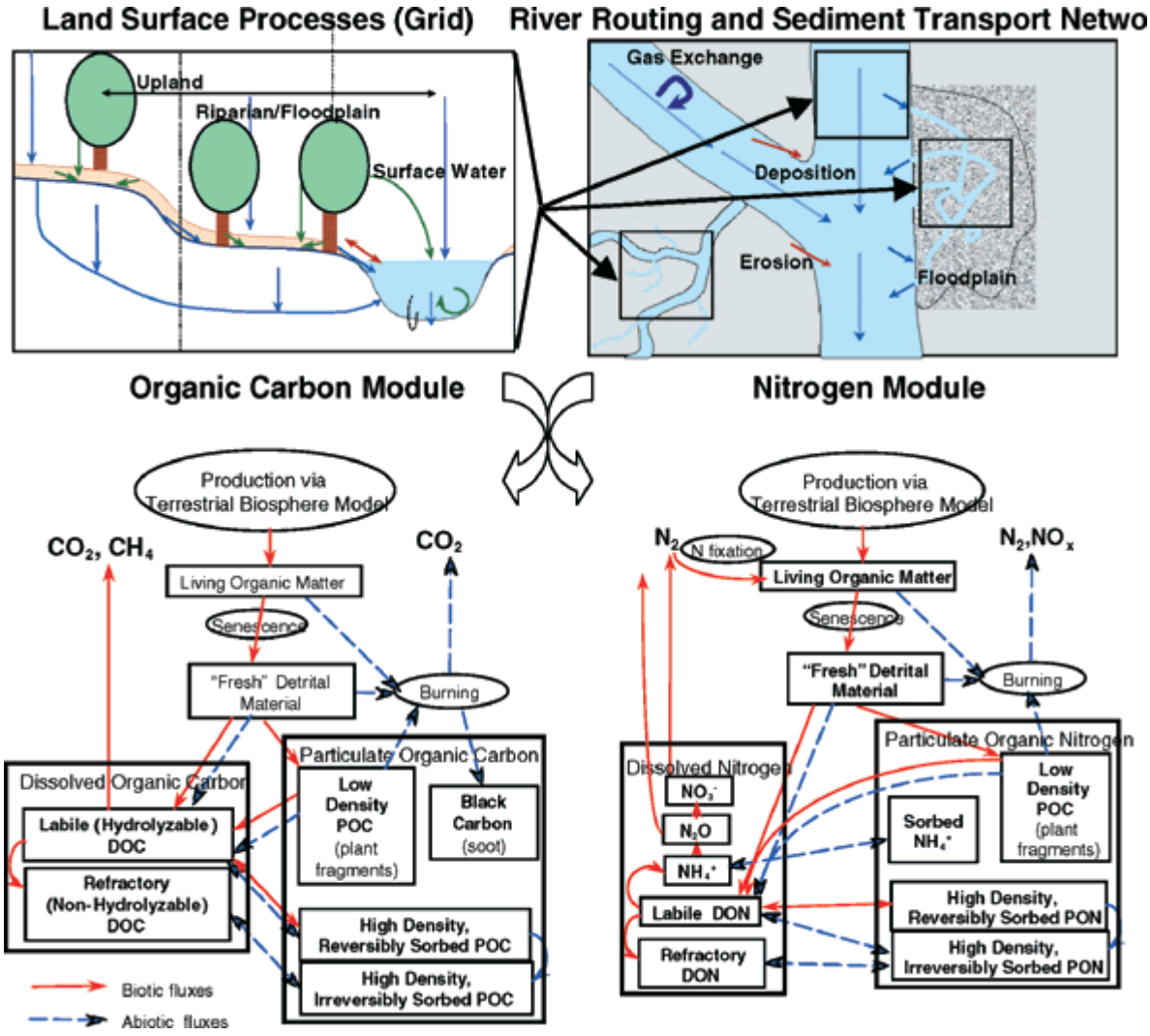

Fig. D.64. Mayorga et al. (2000) proposed an integrated modelling framework for describing the dynamics of organic matter (OM) cycling in mesoscale to large rivers, including *DOC* (dissolved organic carbon), *POC* (particulate organic carbon), *DON* (dissolved organic nitrogen), and *PON* (particulate organic nitrogen) (after Mayorga et al. 2000)

fication. These steps lead to the production of N_2 and N trace gases, removing N from cycling within an ecosystem.

Rivers and the water they carry thus provide a continuously flowing signal, recorded by isotopes, ions and molecules, of the cumulative effects of drainage basin processes such as weathering, oxidation/reduction, gas exchange, photosynthesis, biodegradation and partitioning. This recording is complementary to more classical methods of remote sensing-based on electromagnetic radiation, but is composited over a wider range of time and space scales and includes effects of subcanopy and subsurface processes. Hence an understanding of how these substances are routed from precipitation through their drainage systems to the oceans yields important information on the processes controlling regional-scale hydrological and biogeochemical cycles.

We will now use this framework to summarise the coupled hydrological and biogeochemical dynamics of the Amazon, in a manner that can lead to extrapolation to other systems.

D.5.3 The Amazon Basin: Vargem Grande to Óbidos

The Amazon drainage basin is characterised by areas of extremely high relief (Andes and sub-Andean trough) which transition into regions of low relief (shield areas and alluvial plain). The central Basin and the corridor to the Atlantic are composed of sediments from these formations as well as marine deposits. Over 90% of the sediment which eventually reaches the ocean is contributed by the Andes (Meade 1994). The geological stability of most of the Basin and the high amounts of rainfall have led to the development of a low-gradient topography and highly weathered soils, usually oxisols (mineral soils with an oxic horizon) and ultisols (mineral soils with an argillic horizon), in the region east of the Andes. Early on, the linkage between the geology, biology and hydrology of the Amazon River mainstem was recognised from visually observable features of the waters and was formalised into an Amazon river "typology" by Sioli (1950). This classification consists of visually distinct white-water, clear-water, and black-water rivers.

For the purposes of this paper, we divide the overall Basin into subbasins represented by the primary tributaries and the mainstem floodplain (Fig. D.65). The primary tributary basins range from about 50 000 km^2 to more than 1 Mkm^2, or from large mesoscale to continental scale in area (Table D.25). The Rio Madeira and the Amazon mainstem at Vargem Grande have predominantly Andean origin, with the greatest mean elevation, relief, and slope. The Rio Madeira originates in the Bolivian Andes and then passes across the Planalto Brasileiro and the central plain. The northern tributaries the Rios Içá and Japurá originate in the Andes and cross the sub-Andean trough and central plain to reach the main stem. Of the southern tributaries, the Juruá, and Purús drain the sub-Andean trough and the central plain. All of these rivers are considered white-water rivers, with high sediment concentrations. They drain relatively unweathered soils and geological formations and

Fig. D.65.
The Amazon drainage basin, with primary tributaries indicated. Vargem Grande (*VG*) and Óbidos (*OBI*) are the upstream and downstream ends of the river reach sampled, and Itapeuá (*ITA*) and Manacapurú (*MAN*) are mid-reach stations. The river network is derived from the Digital Chart of the World (DCW) river channel dataset. The attributes of the primary basins are summarised in Table D.25

Table D.25. Attributes of the primary tributary basins of the Amazon River, including the mainstem, tributaries draining from the north, and from the south (Fig. D.65). Vargem Grande (mainstem Solimões just above the confluence with the Rio Içá) represents primarily drainage from the Andes of Peru and Ecuador. Óbidos is the most downstream mainstem station that is routinely measured. To derive consistent river networks and drainage basin boundaries, a new algorithm was developed that creates flow-direction grids from a manually corrected vector cartographic dataset, the Digital Chart of the World; this topography-independend method was created in order to sidestep data problems present in the best available elevation dataset, GTOPO30. The new derived dataset was then used to calculate drainage basin areas, and combined with GTOPO30 to calculate mean basin elevation, relief, percent of basin > 500 m in elevation, and mean slope. Soil texture (mean soil organic C, clay content, and sand content) was calculated from Brazilian RADAM soil maps for the Brazilian Amazon and from the FAO 1° × 1° gridded dataset for the non-Brazilian Amazon. These texture classes are used in hydrology models to estimate field capacity, wilting point, and available water capacity (field capacity minus wilting point) using the texture-based methods of Saxton et al. (1986). Rooting depth (which determines to what depth vegetation can access water) can be specified as a function of soil texture and vegetation type (*sensu* Nepstad et al. 1997)

Basin	Area (10^3 km^2)	Elevation (m)	Relief (m)	>500 m (%)	Slope (%)	Soil org. C (kg C m^{-2})	Clay (%)	Sand (%)	Forested (%)	Precipitation (mm yr^{-1})
Mainstem										
Vargem Grande	1 010	1 040	5 900	39	3.9	11.1	41	39	70	??
Óbidos	4 680	450	5 960	15	1.6	10.0	39	37	79	2 140
Northern										
Içá	120	210	3 470	7	0.4	10.6	45	30	89	2 640
Japurá	260	250	4 180	9	0.9	10.0	39	35	85	2 880
Negro	710	180	2 960	7	0.8	10.2	35	43	81	2 470
Southern										
Jutaí	50	90	150	0	0.1	9.7	35	32	94	2 890
Juruá	220	180	480	1	0.2	9.0	38	27	96	2 350
Purús	360	140	500	>1	0.2	9.3	37	29	93	2 210
Madeira	1 380	500	5 860	17	1.8	10.0	39	40	70	1 870

are characterised as "weathering-limited denudation" by Stallard and Edmond (1983), i.e. the transport processes are more rapid than the weathering processes that are creating materials for transport. Because the transported materials are still rich in more soluble components, the dissolved inorganic load of these waters is also high.

The Rio Negro, the classic black water river, lacks Andean headwaters and drains older, more weathered soils on lower relief surfaces of the Caatinga forest on the Planalto das Guianas, and its major tributary, the Rio Branco, drains a drier savanna region. The Rio Jutaí also has characteristics of black water. The loads that they carry reflect the capacity of transport processes to remove them, so they are characterised as "transport-limited denudation" (Stallard and Edmond 1983). These waters have very low suspended sediment concentrations and are usually tea-coloured in appearance due to a high load of organic acids. The clear water rivers are intermediate between the black and white, including the Trombetas, Tapajós, and Xingú.

The Amazon floodplain, or várzea, is an integral part of the river system, where floodwaters and local runoff regularly inundate the floodplain via an extensive network of drainage channels. Thousands of permanent lakes range in size from less than a hectare to more than 600 km^2, and are typically 6–8 m deep at high water. As the river falls, land is re-exposed and the lakes become isolated from the main channel, with depths decreasing to 1–2 m. Numerous smaller tributaries drain exclusively lowland regions into the main channel or into the floodplain, while large "paranas" act as diversion canals between the main channel, floodplain, and tributaries, with the flow direction often depending on river stage. The upstream reach (Vargem Grande to Itapeuá) is characterised by rapid migration of mainstem and floodplain channels to produce an intricate scroll-bar topography with long, narrow lakes. The middle reach, between Itapeuá and Manacapurú, has a narrow floodplain with fewer lakes than upriver, and is controlled by structural features that constrain the river and allow almost no morphological change. The downstream reach, Manacapurú-Óbidos, has an incomplete levee system, which provides free access for overbank flows to a wide floodplain with a patchwork of wide, shallow lakes.

While large rivers define the fundamental character of the Amazon landscape, they owe their flow and chemical loads to a much denser network of small rivers and streams, at small to mesoscales. In the relatively low-gradient terrain of the Brazilian Amazon, streams follow slow and meandering courses through flat-bottomed valleys. The streams are often bounded by riparian forests whose elevation is similar to that of the streams and lower than that of the surrounding forests or grasslands by as much as several metres. In an area near Manaus, for example, stream density is approximately 2 km km^{-2} (Junk and Furch 1993); and the combined area of the streams and

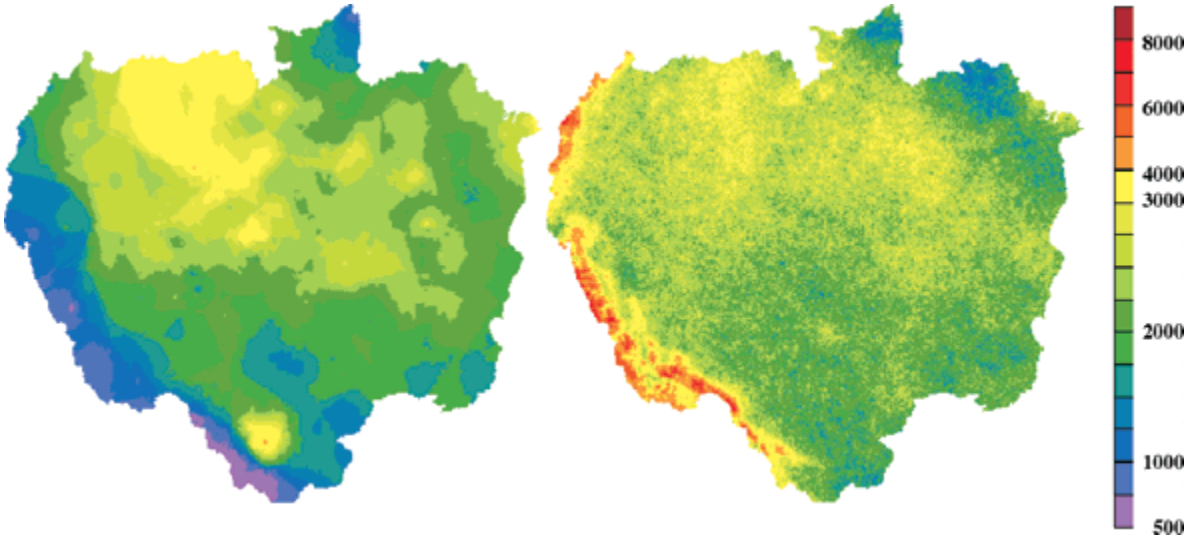

Fig. D.66. Annual rainfall fields (mm yr^{-1}), derived from the gauging network of the Agência Nacional de Aguas e Energia Elétrica (*on the left*) and from an AVHRR satellite index (*on the right*)

riparian zones in the Amazon Basin has been estimated at close to 1 Mkm^2 (Junk and Furch 1993). The hydrology of the small streams is strongly influenced by the surrounding land surface as well as by the upstream reaches. Most of the flow is fed by groundwater discharges, while stormflow occurs as saturation overland flow originating in near-saturation riparian soils. The chemistry of major ions of the streams falls within the general categories of black and clear waters, varying according to the geological characteristics and soil properties of their catchments.

D.5.4 Hydrology of the Amazon River System: A Mainstem Perspective

D 5.4.1 Patterns of Rainfall

As most recently summarised by Marengo and Nobre (2001) and Nobre (compare Chapt. A.6), the Amazon region is characterised by a strong annual cycle of rainfall, with varying patterns across the Basin (Fig. D.66). Annual variation in rainfall is linked to annual changes in the large-scale upper-air circulation. Although the sun largely controls the timing of the annual cycle of rainfall, rainfall in different parts of the Basin is triggered by different rain-producing mechanisms. Diurnal deep convection resulting from surface warming is most prevalent in central Amazônia, while deep convection in northern Amazônia is related to the Intertropical Convergence Zone and the moisture transports from the Atlantic. Instability lines originating near the mouth of the Amazon River can initiate rainfall in northern Amazônia, while convective activity at meso-scale and large-scale, associated with the penetration of frontal systems in south/south-east Brazil, can reach western southern Amazônia. Southern Amazônia has distinct dry and rainy seasons, with a maximum of rainfall in January-to-March. In the northern and central regions there is almost no dry season, but approaching the Equator there is a distinct maximum in spring and a "suppressed" maximum in the autumn. The north-west region (basins of the Rios Negro, Içá, and Japurá) has high rainfall, with more than 3 600 mm yr^{-1}, and peaks in April-to-June. The central part of Amazônia around 5° S averages about 2 400 mm yr^{-1}, while the region near the mouth receives more than 2 800 mm yr^{-1}. The extremely high and localised values of precipitation occur in narrow strips along the eastern side of the Andean slopes, reaching upwards of 7 000 mm yr^{-1}.

While these broad patterns of precipitation are accurate, a problem for modelling exists with the reconciling of predictions with sufficiently accurate measurements. Precipitation gauges in the north-west and especially along the eastern slopes of the Andes of Peru and Ecuador are so sparse as to render estimates of seasonality relative to observed river hydrographs problematic. Current gauge-based estimates of precipitation in the Solimões basin at Vargem Grande would require unrealistically-low evapotranspiration (cf. Salati et al. 1979) to match observed discharge at that station (Richey, unpublished data).

D.5.4.2 Mainstem and Tributary Hydrographs

The most striking features of Amazon River discharge are its magnitude and its highly damped hydrograph (Fig. D.67). The Amazon mainstem discharges between Vargem Grande and Óbidos are determined by inputs

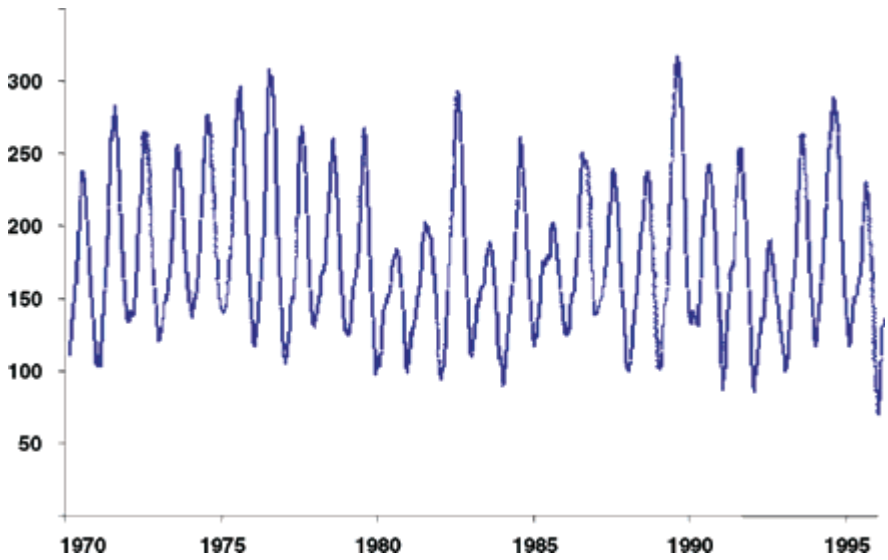

Fig. D.67.
Amazon discharge at Óbidos ($m^3 s^{-1} \times 1000$). Óbidos, as the last gauged station on the Amazon mainstem, represents the runoff of 4.6 Mkm^2 of drainage basin, and is considered the defining point for input to the ocean (with the addition of the Rios Xingú and Tapajós)

from upstream, from the primary tributaries and local rivers, and from exchange with the várzea. Though differences in stage of 7–10 m are common along the main stem, there is only a twofold to threefold difference between low and high discharges. The damped hydrograph of the main stem reflects in part the offset input from tributaries and along the channel. The peak flows from the northern and southern tributaries are typically three months out of phase as a result of the seasonal differences in precipitation (Fig. D.68).

As summarised from Richey et al. (1989a, 1990) and more recently by Carvalho and da Cunha (1998), the Amazon at Vargem Grande is primarily Andean water, with average minimum and maximum discharges of 20 000 $m^3 s^{-1}$ and 60 000 $m^3 s^{-1}$. The average annual discharge of the tributaries includes the Içá (9 000 $m^3 s^{-1}$), Japurá (19 000 $m^3 s^{-1}$), Jutaí (3 000 $m^3 s^{-1}$), Juruá (8 000 $m^3 s^{-1}$), Purús (12 000 $m^3 s^{-1}$), Negro (28 000 $m^3 s^{-1}$), and Madeira (31 000 $m^3 s^{-1}$). Thus the main channel of the Amazon River at Óbidos receives input from major and minor tributaries draining an area of 4.2×10^6 km^2, with low and high flows average 100 000 $m^3 s^{-1}$ and 220 000 $m^3 s^{-1}$, respectively. The total Amazon input to the Atlantic (Óbidos plus the Rios Tapajós and Xingú, represents a mean annual input of about 210 000 $m^3 s^{-1}$.

In-channel storage and especially floodplain storage and exchange influence the mainstem hydrograph and was shown to be essential to any modelling study of the river (Richey et al. 1989a; Vörösmarty et al. 1989). The increase in storage on the floodplain over the 8-month period of rising water is greatest during the mid-rising water phase in the upriver reach of the main stem, ap-

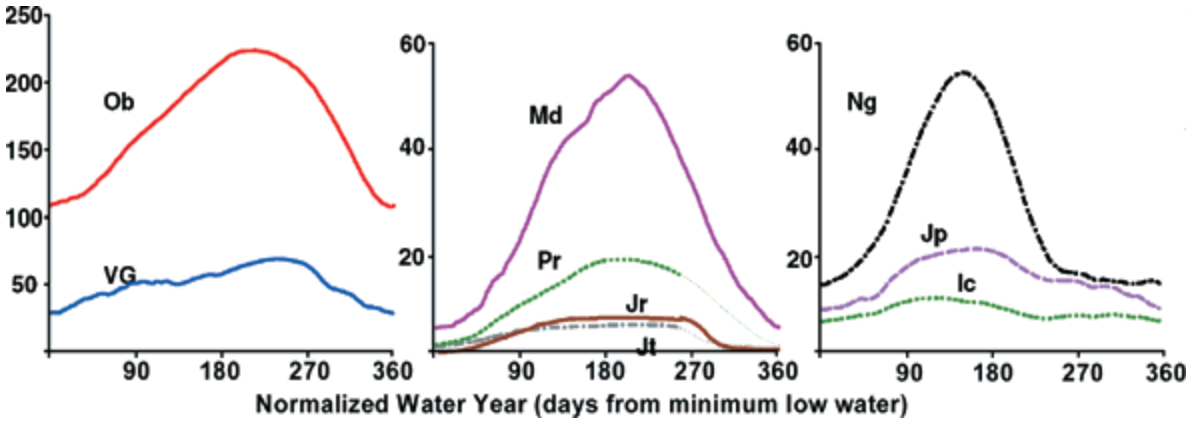

Fig. D.68. Composite discharge hydrographs ($m^3 s^{-1} \times 1000$) of the primary Amazon tributaries. Each hydrograph is for the water year of the respective tributary, which starts on the date indicated in parentheses (as calculated from mean discharge, 1972–1990). The Içá (*Ic*, Jan 31), Japurá (*Jp*, Jan 31), and Negro (*Ng*, Jan 31) are predominantly in the Northern Hemisphere, while the Jutaí (*Jt*, Oct 9), Juruá (*Jr*, Sep 18), Purús (*Pr*, Oct 19), and Madeira (*Md*, Sep 25) are in the Southern Hemisphere. Mainstem stations include Vargem Grande (*VG*, Sep 10; essentially representing Andean drainage) and Óbidos (*Ob*, Oct 19). The differences in timing represent the seasonality of the respective basins, established in large part by fluctuations in the Intertropical Convergence Zone

proaching 15 000 $m^3 s^{-1}$, with maximum rates in the midriver and downriver reaches of 3 000 $m^3 s^{-1}$ and 9 000 $m^3 s^{-1}$, respectively. The decrease in storage during the 4-month falling water period is greatest during mid-falling water, ranging from –18 000 $m^3 s^{-1}$ upriver to –8 000 $m^3 s^{-1}$ at midriver. Water exchange between the várzea and main channel ranges from 3 000 $m^3 s^{-1}$ during the dry season to 7 000 $m^3 s^{-1}$ during the wet season in the up- and downriver sections; midriver flows are about half of these values. Overall, exchange is greatest during early-falling to mid-falling water in the upriver and downriver reaches, with a net flow from the floodplain to the main stem of about 20 000 $m^3 s^{-1}$. Net exchanges are generally lower in the midriver reach, where the area of the floodplain is relatively small. Therefore, water derived from local drainage constitutes a significant component of the water budget of the main stem. These flows correspond to about 30% of the flow at Itapeuá, and cumulatively to about 25% of the flow at Óbidos.

The predominant interannual variability in Amazon discharge occurs on the two to three year time scale, and oscillations in the hydrograph are coupled to the El Niño-Southern Oscillation cycle (ENSO), with a lag of about five months (Richey et al. 1989b). The oscillations of river discharge predate significant human influences in the Amazon Basin, and reflect both extra-basin and local factors. Climate records and general circulation model calculations suggest that interannual variations in the precipitation regime and hence discharge of the Amazon are linked to changes in the general circulation of the atmosphere over the tropical Pacific Ocean associated with ENSO. Qualitatively, the months of maximum pressure anomalies (Southern Oscillation negative phase) correspond to ENSO warm events and precede the negative flow anomalies in most cases. Major ENSO events, e.g. 1925–1926 and 1982–1983, are reflected in pronounced low discharges. The converse effect, high discharge associated with the Southern Oscillation positive phase, is also apparent. Only a portion of the variance in the discharge regime is linked to the ENSO phenomenon. Relations between runoff and precipitation are not straightforward, due in part to the carry-over storage ("basin-memory effects") typical of large catchments. Local climate influences, such as the boundary layer convergence mechanisms and the steady progression of individual fronts and air mass boundaries characteristic of the region, contribute to discharge variability.

In summary, the damped hydrograph of the mainstem reflects the large drainage basin area, the three-month phase lag in peak flows between the north- and south-draining tributaries related to seasonal differences in precipitation, and the large volume of water stored on or passing through the floodplain. Patterns of interannual variability indicate that considerable caution must be exercised in determining anthroprogenic impacts, particularly with the use of short-term records over large areas. Conversely, it would be difficult to uniquely identify a deforestation effect in the highly damped discharge regime of the Amazon River mainstem (with records dating back to 1903). The likelihood of linkages between the Amazon Basin and large-scale atmospheric circulation reinforces the importance of determining the factors controlling the hydrology of the Basin in the face of extensive land-use change. A rigorous analysis of the regional-scale hydrology of the Basin using field measurements and remote sensing integrated through realistic, physically-based modelling must be considered as the long-range goal for assessing and managing sustainable development in the Basin.

D.5.4.3 Models of Amazon Water Movement

The next major challenge is to relate the mainstem and tributary flow regimes to the antecedent conditions in the respective tributaries via spatially-explicit hydrological modelling. For example, a dynamic water balance model developed by T. Dunne (University of California Santa Barbara, pers. comn.; see also Vörösmarty et al. 1996a; Costa and Foley 1997) has been used to translate precipitation into runoff. As do many models of this type, it uses a tipping-bucket conceptualisation of moisture and moisture fluxes in the root zone. The tipping bucket assumes that all precipitation that enters the soil (assuming a fraction of precipitation runs off as overland flow) remains in the root zone until the moisture content reaches field capacity. At this point excess infiltrate is assumed to drain instantaneously to groundwater storage. Moisture content in the upper zone decreases only through transpiration, with transpiration ceasing when the moisture content drops to the wilting point. Evapotranspiration is calculated using a Priestley-Taylor formulation, where net radiation is the dominant forcing variable (under humid conditions). As such, the model is able to account for stomatal resistance to transpiration, as well as interception, canopy evaporation, and overland flow (which reduces possible additions to soil moisture). The translation of runoff from a cell to a downstream node that could be compared to existing gauging records is calculated using constant travel times and a convolution integral.

This model was applied to the Amazon at a spatial resolution of $0.05° \times 0.05°$ (longitude by latitude). Input parameters were re-sampled to this resolution with a binary integer image format from data layers in both vector and raster data sources in a modelling environment managed by a GIS (Geographic Information System). For the relatively high-resolution models used here, surface meteorological stations by themselves are far too sparse and global datasets are far too coarse. Hence a combina-

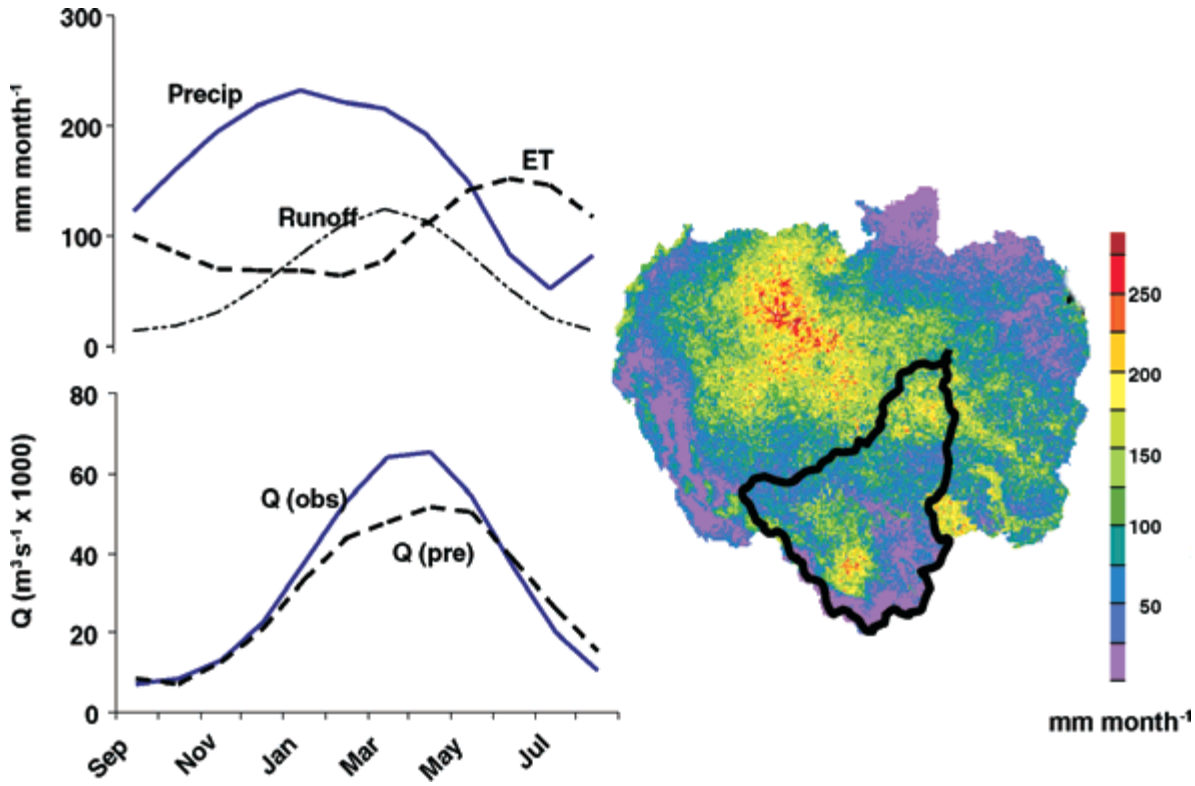

Fig. D.69. Hydrology model results for one time period for the whole basin, with reference to the specific discharge for the Rio Madeira (basin outline *indicated*)

tion of field point data and satellite-derived information. A time series of daily data from the Advanced Very High Resolution Radiometer (AVHRR) Global Area Coverage (GAC, about 5 km) from the NOAA-7, -9, and -11 satellites was used in conjunction with surface data to create fields of precipitation, solar radiation and temperature. The model performs reasonably well in representing the dynamics of these rivers. For example, the model hydrograph captures the phase and generally the amplitude of the Rio Madeira, which varies from a low of about 5 000 $m^3 s^{-1}$ to a high of about 70 000 $m^3 s^{-1}$ (Fig. D.69). The underestimate is thought to be due to difficulties in accurately estimating the amount of precipitation.

D.5.5 River Chemistry

A significant challenge in understanding the biogeochemical dynamics of the Amazon Basin in a systematic manner surrounds an optimal sampling strategy and means by which to sensibly integrate the results. The Basin is obviously very large, making it difficult to perform routine synoptic sampling. Because the hydrographs of the tributaries and mainstem stations may be out of phase with each other by up to three months, each sample point occurs at a different point on the hydrograph of the respective river, even if the samples are collected on the same day. Furthermore, a volume of water travels downstream in channels from 1–3 m s^{-1}, or 100–300 km d^{-1}, so translocation of sampling points can be problematic. To solve these problems, the CAMREX (Carbon in the Amazon River Experiment) programme conducted a series of sampling cruises between Vargem Grande and Óbidos during the period 1982–1991, using the sampling protocol of Richey et al. (1986).

D.5.5.1 A Synoptic View of Chemical Profiles

We hypothesise that a good first-order descriptor of integrated riverine chemistry is the distribution of chemical concentrations with respect to discharge and, more specifically, to the rising and falling limbs of hydrographs. To account for differences in hydrograph timing on the respective tributaries, annual average discharge hydrographs from each station can be calculated, taking the mean discharge for each day from the period of record, starting from minimum low water for each tributary (Fig. D.70). These hydrographs represent the highly damped signal of multiple upstream events, aris-

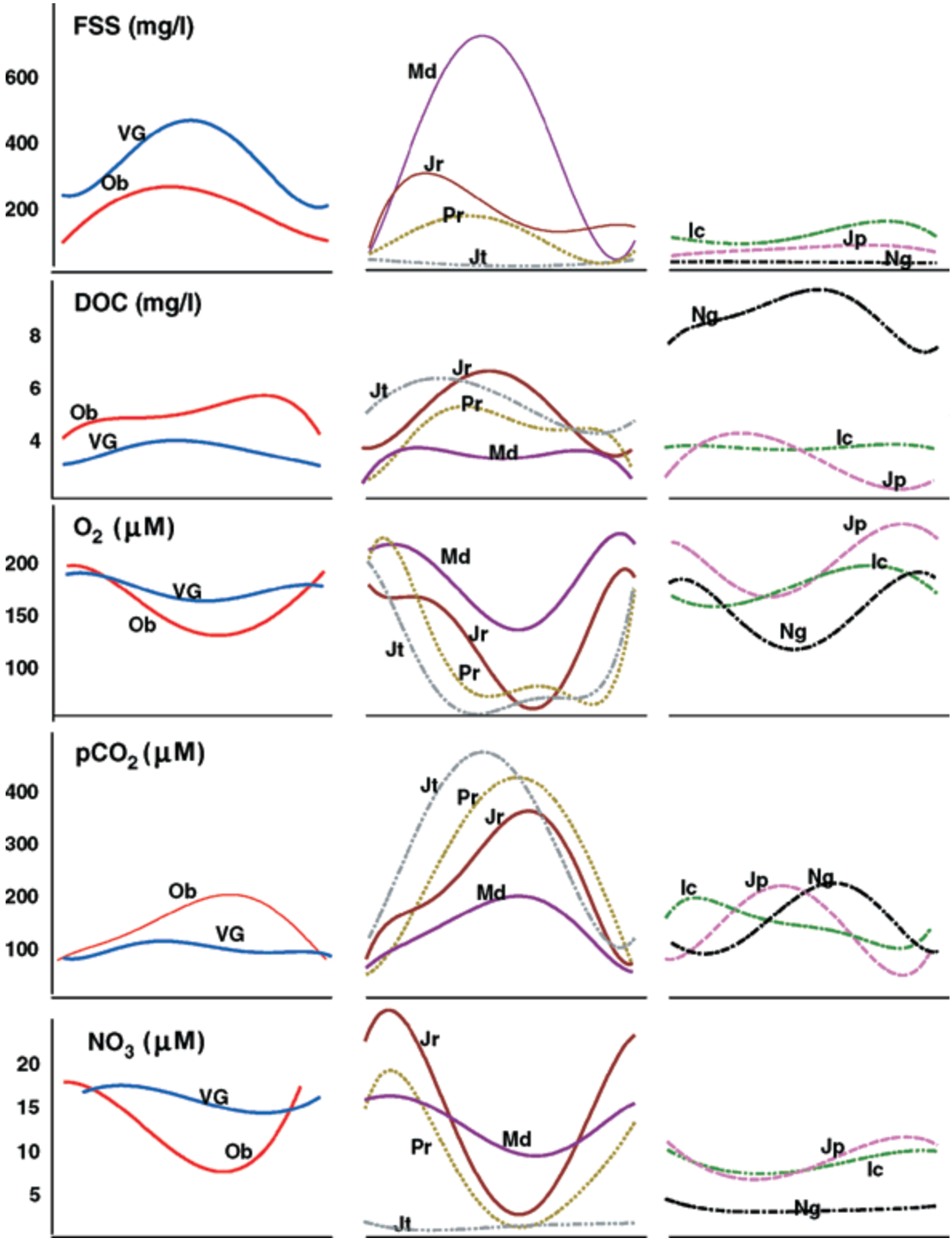

Fig. D.70. Composite chemical hydrographs for the primary tributaries and mainstem stations (as described in Fig. D.68). Chemical species include fine suspended sediments (*FSS*, < 64 mm), dissolved organic carbon (*DOC*), dissolved carbon dioxide (pCO_2), dissolved oxygen (O_2), and nitrate (NO_3)

ing from the mixing of separate tributary inputs and along-channel processes. Concentrations of all chemical species were generally more variable over the hydrograph relative to the mainstem, and differed considerably from one tributary to the next.

Over 95% of the particulate material transported by the Amazon River is carried in suspension, with computed bedload transport rates only 1–2% of the total sediment load (Dunne, pers. comn.). Most of the suspended fraction is carried as fine sediments (< 64 μm). Peak fine suspended sediment concentrations occur about half way up the rising limb of the hydrograph. The mainstem at Vargem Grande has a peak of fine suspended sediment concentration of about twice that of Óbidos. The southern tributaries contribute by far the most sediment, led by the Rio Madeira (peak values approaching 700 mg l^{-1}), followed by the Rios Purús and Juruá. In all these tributaries, the peak of fine suspended sediment occurs on the rising hydrograph. In contrast, the northern tributaries have lower concentrations, showing slight peaks on the falling limb. As the weight-percent of C and N to sediment is quite constant (Hedges et al. 1994, Richey et al. 1990), it may be inferred that the dynamics of the transport of particulate organic matter transport is governed primarily by the movement of the bulk mineral sediment.

Approximately 60–90% of the total dissolved inorganic carbon exists as bicarbonate at the average Amazon pH values of 6.5–7.2, with the balance being dissolved CO_2 gas; carbonate alkalinity is virtually zero (Richey et al. 1990). The mainstem is supersaturated with respect to CO_2 in the atmosphere by 10 to 20 times. Dissolved CO_2 increases almost precisely with the hydrograph, from 100 to 200 μM, with an overall mean of 130 μM. Because of the supersaturation, the total annual evasion of CO_2 from the river to the atmosphere is equivalent to about 50% of total dissolved inorganic carbon export, and is derived primarily from *in situ* respiration. Mainstem dissolved O_2 has the exact inverse distribution from pCO_2. It is 50% to 80% undersaturated relative to the atmosphere, and has its minimum at peak high water. Nitrate and dissolved organic N (not shown) together account for 50% of the total N in the mainstem, while NH_4 is present only at detection-limit concentrations. The overall mean NO_3 is 12 μM, with a seasonal distribution mirroring O_2. The annual average flux of total N out of the reach at Óbidos is 3 Tg yr^{-1}, of which 44% is fine particulate N, 27% is NO_3, 26% is dissolved organic nitrogen, and 3% is coarse particulate N.

Dissolved organic carbon at Óbidos is enriched by 1–3 mg l^{-1} relative to Vargem Grande. The highest concentrations are found in the Negro, followed by the Jutaí, Juruá and Purús (Richey et al. 1990). The rise and fall of dissolved organic carbon generally tracks the hydrograph. The annual average export of dissolved organic carbon at Óbidos of 22 Tg yr^{-1} is derived primarily from the Negro (31%) and Vargem Grande (20%). Várzea drainage contributes about 17%. Dissolved CO_2 at Óbidos at high water is about twice that of Vargem Grande, while O_2 is lower. The southern tributaries have very elevated levels of pCO_2 and commensurately reduced levels of O_2 relative to the mainstem, especially the Jutaí, Juruá and Purús, all concurrent with the phase of the hydrograph. Values in the northern tributaries and the Madeira tend to be more consistent with the mainstem. NO_3 is reduced at Óbidos relative to Vargem Grande, and show dramatic depletions in the Juruá and Purús and to a lesser extent the Madeira over the course of the hydrograph. The Negro and the Jutaí both have little NO_3. Overall, inputs of NO_3 to the mainstream are more or less evenly divided between Vargem Grande (45%) and the sum of the tributaries (49%).

On the basis of these profiles, we can reconsider the basic groupings of the tributaries relative to the original typologies of water colour. There is a clear gradation in the relative "whiteness" of tributaries, from the high sediment Madeira to the mainstem Solimões at Vargem Grande, then to the Juruá, Purús, Içá and Madeira. The Jutaí often appears as "black" as the Rio Negro, has significant levels of dissolved organic carbon (though not as high as the Negro) and, like the Negro, has low NO_3. However it has higher levels of pCO_2 and lower O_2 than does the Negro. Perhaps the most intriguing feature in the tributaries is how dramatically and how in synchrony pCO_2 increases and O_2 and NO_3 decrease with the respective hydrographs. What has not been resolved at this time is whether this phenomenon is due to differences in inputs from land, in-channel processes, or local floodplain dynamics.

D.5.5.2 In-river Dynamics

The key to understanding biogeochemical transformations that occur in a large river system and can be summarised by the distributions such as those represented in Fig. D.70 is to understand the processes controlling the source, transport dynamics, and fate of organic matter and nutrients. Extensive work on the transport and mineralogy of sediment within the Amazon River system has shown that most river-borne particles are derived from the Andes but, due to erosion/deposition cycles, they clearly do not pass unaltered through the river system (Johnsson and Meade 1990; Meade et al. 1985; Meade 1994; Mertes et al. 1993, 1996; Martinelli et al. 1993). The hydrological and material transfer properties of a floodplain determine the degree to which biological and chemical processing imparts a signal on materials derived from either upland or main channel sources. At the most basic level, the hydrology of different water types – as they enter the floodplain from rainfall, local tributaries, and the main channel – is primarily a result of the timing of the supply with respect to other sources and the topography and soils of the floodplain.

Results of in-channel process modelling indicate even stronger ties between the mainstem and the floodplain than previously expected. Field measurements indicated that over 80% of the suspended sediment that is introduced to the floodplain from either the main channel or local tributaries is deposited on the floodplain surface (Dunne et al. 1998). On the other hand, substantial amounts of sediment enter the main channel via bank erosion. Estimates of the contribution of floodplain soils and sediment to the main channel flow indicate that approximately 1.5 billion tons of sediment are eroded annually (Dunne et al. 1998). Conservatively, these values indicate that the exchange of bank materials at least equals the discharge of sediment passing Óbidos annually (1.2 billion tons). It is thus unlikely that an individual particle travels through the study reach without intermediate storage. From ^{14}C and mineralogy data, it is possible to estimate that in the mainstem, a typical particle passes through the floodplain several times and that, given the pattern of channel migration, the floodplain in most reaches is recycled over a few thousand years. Measurements of the C, N, and ^{13}C of suspended sediments and floodplain sediments in different environments directly confirm the floodplain imprint (Martinelli et al. 1993; Quay et al. 1992).

Similarly, the distributions of the bioactive elements are strongly influenced by *in situ* and lateral processes, even in very large rivers. A sequence of processes controlling in-stream transformations, including in-stream metabolism, sediment transport, and gas exchange has been summarised (Richey et al. 1990; Richey and Victoria 1993; Devol et al. 1995; Devol and Hedges 2001; Quay et al. 1992, 1995; Bartlett et al. 1990; Benner et al. 1995; Amon and Benner 1996). These measurements indicate that although strongly heterotrophic, the mainstem Amazon is substrate-starved. Within-river respiration appears to be largely at the expense of a limited pool of moderately reactive biochemicals dispersed among highly degraded dissolved and particulate forms. The river is in quasi-steady state with respect to respiration balancing gas exchange.

To evaluate the relative importance of different factors on controlling these distributions, Richey and Victoria (1996) modelled the changes in O_2, pCO_2, NO_3, and dissolved organic carbon in a volume of water as it moves downstream, in terms of the respective source and sink terms. Observed dissolved organic carbon profiles can be predicted only with the floodplain as a source of dissolved organic carbon, and with about 60% of respiration being derived from dissolved organic carbon. Hence there is the clear implication that net dissolved organic carbon is not conservative. Downstream levels of NO_3 could be explained only through NO_3 released by *in situ* mineralisation. The conclusion is that exchanges between the floodplain and mainstem have a significant, if not dominant, impact on the metabolism of the mainstem.

D.5.5.3 Organic Geochemical Signatures

The previous discussion emphasized the distribution of the important and common "bulk" chemical parameters. Much more can be learned about the sources, chemical condition and fate of the material in transport by considering the more detailed chemical composition of these materials (Fig. D.71). The organic geochemical composition of the suspended sediments represents a sequence of processes originating with the fixation of carbon on land through degradation and mobilisation pathways.

Comparisons between the main fractions of organic matter (coarse, fine, and dissolved) and on the role of partitioning of organic materials between water and mineral surfaces within the river system (e.g. Hedges et al. 1986a,b, 1994) is illuminating. Comparison of the main fractions confirms that coarse particulate organic material appears to consist of relatively fresh tree leaves. Although both the fine particulate organic material and dissolved organic material fractions are highly degraded, fine particulate organic material is richer in nitrogen than dissolved organic material and contains 5–10 times more total amino acids. This trend extends to the molecular level, where fine particulate organic material is characterised by higher ratios of nitrogen-rich acidic amino acids versus carboxyl-rich acidic amino acids. This concentration of nitrogen in fine particulate organic material fits a scenario in which dissolved leaf degradation products are selectively partitioned onto negatively charged particles (as nitrogen imparts a local positive charge to organic molecules). In addition, measurements of ^{14}C age indicate that fine particulate organic material is the fraction with the longest maximum residence time and thus moves most slowly through the Basin. The ^{14}C age of bulk dissolved organic material is close to the modern atmospheric signature, which suggests that its diagenesis and transport times are surprisingly short. Comparison of tracers between the chemical fractions highlights the differences between the different size classes of organic matter, and the differences between basins. Although traditional humic extracts on Amazon samples have been done (Ertel et al. 1986), the information contained within the biochemical analyses provides a more coherent picture of the biogeochemical cycling of organic matter in the Amazon.

D.5.5.4 Dynamics of Floodplains

The várzea represents a complex and integral part of the biogeochemical cycles and foodwebs of the Amazon River system (Araújo-Lima et al. 1986). Portions of the white-water rivers remain in fixed channels while others meander, creating new surfaces for the colonisation of vascular plants. Biological activity is greatest on

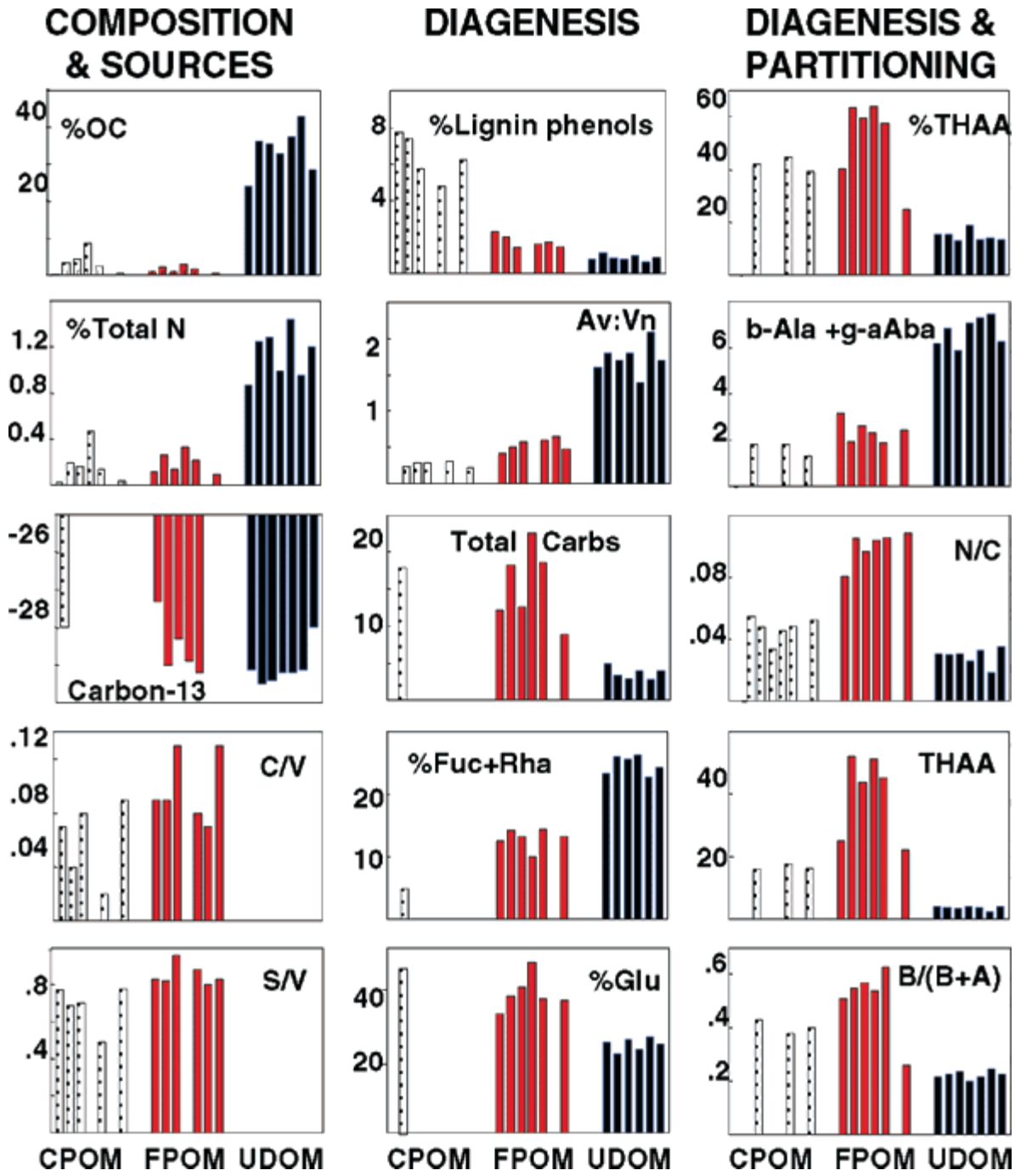

Fig. D.71. Significant trends in organic geochemical parameters (based on data from Hedges et al. 1994). *X*-axis parameters (each bar represents the average of one major tributary to the Amazon mainstem): *CPOM:* coarse particulate material (> 64 mm); *FPOM:* fine particulate material (0.2–64 mm); *UDOM:* ultrafiltered dissolved material (1000 Daltons to 0.2 mm). *Y*-axis parameters and the attributes they represent (*top* to *bottom*, *left* to *right*): *%OC* and %Total Nitrogen reflect bulk trends in carbon and nitrogen. ^{13}C-isotopes are source indicators that can be used in terrestrial systems to distinguish between organic matter produced at different altitudes, and sometimes between pollutants and natural compounds. Lignin Phenols (next 4 panels), released during CuO oxidation of terrestrial plants, allow discrimination between many trees and grasses. Cinnamyl/Vanillyl (*C/V*), Syringyl/Vanillyl (*S/V*), and Vanillic Acid : Vanillin (*Av : Vn*) plots indicate source changes and fungal degradation. Carbohydrates (next 3 panels) provide information on the diagenetic "age" of organic matter and discriminate between bacterial and plant sources. High percentages %Fucose + Rhamnose (*%Fuc+ Rha*) are associated with highly degraded material. Of the amino acids (next 5 panels), total hydrolyzable amino acids (*THAA*) are general source and reactivity indicators, yield and compositional data are indicative of reworking, degradation and reactivity. High values of % b-Alanine + g-Aminobutyric acid (*%b-Ala + g-aAba*) and low values of *B/(B + A)* are indicative of diagenetic activity

the floodplains of white-water rivers, and the activity is tied to the cycle of flooding. Main communities on the floodplains are forests of flood-tolerant trees, non-forested lands that alternate between grasses during low-water and floating aquatic vascular plants during high-water, and open water lakes that expand as the floodwaters rise (Junk and Furch 1993).

Along the mainstem Amazon, flooding follows a three-stage pattern, with water entering the floodplain first through the deepest levee breaks, then through shallower levee breaks, and finally by overtopping the levees (Mertes et al. 1996). As these stages progress, water on the floodplain becomes increasingly similar to that of the main channel and less like the local drainage water. Gradients in water properties from river to local characteristics can often be observed across the floodplain. Trees on the floodplain grow mostly during low water periods and many drop their leaves during inundation. In contrast, phytoplankton in the lakes flourish after river water enters the floodplain and supplies nutrients for growth (Fisher and Parsley 1979). Phytoplankton communities in various floodplain lakes have been found to be limited by N only and by N and P (Zaret et al. 1981; Forsberg et al. 1988). The productivity of these systems can be quite high, as much as 25 t C ha^{-1} yr^{-1} in the herbaceous communities (Junk and Piedade 1993), ~ 16 t ha^{-1} yr^{-1} (Junk 1985) in the floodplain forest, and 3 t ha^{-1} yr^{-1} in the phytoplankton community of a lake (Schmidt 1973).

Much of the organic matter produced on the floodplain is also degraded there. Decomposition during the inundation phases includes a significant anaerobic component. For instance, floodplain lakes are often stratified with an anoxic lower layer, and low oxygen conditions also develop in the waters of the flooded forests and macrophyte beds. Methane fluxes have been measured during inundation in all the main vegetation communities on the Amazon floodplain. The magnitude of methane production within the floodplains has been characterised by numerous researchers, who estimate that it is the source of 5–10% of the total global CH_4 flux from wetlands (Devol et al. 1990; Bartlett et al. 1990). The majority of the flux is carried by ebullition, so that the areas of methane oxidation in the waters are bypassed.

D.5.6 Potential Impact of Anthropogenic Change on the River System

The diverse natural ecosystem of Amazônia supports a large resource-based economy. Deforestation for lumber and agriculture has made perhaps the greatest impact on Amazon ecosystems. Extensive road-building during 1960–1980 converted large areas of forest to crop land and cattle pasture. Between 1978 and 1988 the amount of deforested land in Amazônia increased from 78 000 to 230 000 km^2 (Skole and Tucker 1993). Mining and extraction of gold and aluminum have impacted the chemistry of certain Amazon River subcatchments, resulting in elevated concentrations of mercury in the river, sediments, fish and some humans (Martinelli et al. 1988, Roulet et al. 1998). Another developmental activity that has directly impacted the Amazon River system is dam building to produce inexpensive electricity to attract investment (Bunyard 1987). The reservoirs they created also produce methane gas that is eventually emitted to the troposphere.

As discussed by Richey et al. (1997), changes in land use would have indirect consequences through modification of uplands and through direct impact of the river corridors themselves. Changes in the uplands can affect the lower-lying river corridors by altering the fluxes of water, sediment, and biological materials transferred to them. Intact riparian zones and floodplains could buffer upland land-use changes. But the riparian zones and floodplains in the river corridors of the Amazon are also undergoing changes that will affect their nutrient dynamics and buffering ability. The floodplains of the Amazon and some of its major tributaries support important fisheries and are a source of easily accessed timber and fertile soils that can be used during the dry season for agriculture and cattle ranching. Deforestation and pasture creation has already occurred to a large extent in the floodplain of the eastern Amazon mainstem. The riparian areas of small streams are often subjected to the same deforestation and agricultural practices as the upland areas. The general response of these systems is decreased retention or filtering of water and materials. This may include decreased anaerobic processing and trace gas production. Without this filtering system, the rivers may carry larger loads of organic carbon and nutrients to downstream areas. One possibility is the enhancement of primary production downstream due to the increased nutrient loads. In general, rivers will respond with differing magnitudes and lags to natural or human perturbations depending upon the processes involved and the downstream transfer rates.

Even if the Basin undergoes massive deforestation, it will still be very different in character than many of the river basins of the developed world. Many of these other basins have drainage networks that have been channelised and cut off from the floodplains, agricultural lands that have been "reclaimed" from wetlands, and large loads of nutrients from fertilisers and anthropogenic chemicals. Over time, the Amazon may take on some of these characteristics.

D.5.7 Towards a Synthetic Model of Drainage Basins

Overall, we can hypothesise that the quantity and composition of dissolved and particulate bioactive materials

in a parcel of water at any downstream node in the river system is predictable as the product of a common set of processes which occur differentially according to upstream conditions of relative topography, soil organic content and texture, water residence time, and floodplain extent. That is, it should be possible to represent the chemical attributes of any geographic element in the Basin based on the mix of fairly simple properties, regardless of whether it is in the upper Rio Madeira or lower Rio Negro. The downstream chemical hydrograph at the mouth of that tributary is then a function of the chemical source and downstream routing. Within-channel processes can significantly modify the river chemical profile.

Although the model of Fig. D.64 is not yet complete, it is a vision of how to:

- Evaluate our understanding of how biogeochemical and physical processes integrate in a river basin;
- Quantitatively constrain the importance of geochemical and physical processes and predict compositions and fluxes of bioactive elements at inaccessible locations and for different land-use and climate change scenarios; and,
- Improve our ability to infer upstream landscape environments and sequence of processes from observed biogeochemical signatures within a parcel of water.